MATERIALE PLASTICE
https://revmaterialeplastice.ro
https://doi.org/10.37358/Mat.Plast.1964

Crack Propagation for Glass Fiber Reinforced Laminates Containing Flame Retardant: Based on Single-Edge Tensile Loading

ZHAO CHANGFANG[1] (ORCID: 0000-0002-5454-0913), **REN RUI[2], WEI YI[3], YANG GUANG[1], HE BIN[4], ZHANG KEBIN[1], ZHONG JIANLIN[1]***
[1]School of Mechanical Engineering, Nanjing University of Science and Technology, Nanjing 210094, China
[2]Marine Design and Research Institute of China, Shanghai, 200011, China
[3]Jiangsu Xingque Technology Co., Ltd, Danyang, 212300, China
[4]Key Laboratory for Soft Chemistry and Functional Materials, Nanjing University of Science and Technology, Ministry of Education, Nanjing 210094, China

Abstract: *Research on crack propagation for fiber reinforced composites containing flame retardant is rare. The micro-cracks propagation is a reason for delamination and debonding failure of fiber reinforced composites. To study the crack propagation of continuous glass fiber reinforced epoxy resin laminates that contained ammonium polyphosphate flame retardant (GFRP-APP), the quasi-static single-edge tensile loading (SETL) experiments for the end-notched GFRP-APP specimens were carried out by MTS universal electronic testing machine. The crack propagation of the end-notched 90° GFRP-APP specimen includes two types, both of which belong to opening type (mode I). Namely, one type is mode I multi-cracks propagation without preexisting crack, and the other is mode I fiber bridge propagation with preexisting crack. The intralaminar fracture toughness along fiber direction of GFRP-APP is approximately 4.2 N/mm, which is calculated by area method. The opening displacement-tensile force curves can be divided into three stages for 90° GFRP-APP specimen without crack, i.e., crack gestation, crack birth and crack propagation. However, the 90° GFRP-APP specimen with crack not contains the crack birth stage. Additionally, the microscopic morphology for the fracture face of pure epoxy resin and GFRP-APP, and the phase analysis for GFRP-APP were performed by scanning electron microscope (SEM), X-ray diffraction (XRD) and energy dispersive spectrometer (EDS). As a conclusion, the pores and interfaces in materials were the guiding factors of micro-crack propagation, and the ammonium polyphosphate flame retardant particle contributed extra interfaces.*

Keywords: *crack propagation; fracture toughness, ammonium polyphosphate, glass fiber, epoxy resin*

1. Introduction

Fiber reinforced plastic composites (FRPs) are one of the most popular advanced composites in recent years [1], which can be used as functional materials to prepare functional structures. The specific stiffness, specific strength, specific energy absorption and other mechanical properties of FRPs are excellent [2], and the FRPs are widely used in various industrial fields, such as aerospace industry, automobile industry, weapons and military industry [3]. Moreover, with further research on FRPs, its role had transferred from the secondary bearing structure to the main bearing structure. Laminate structures are the most commonly used and cheapest product of FRPs. However, the intralaminar performance of laminates is relatively poor due to micro-cracks, thereby the crack propagation becoming the main failure mode. The micro-cracks will reduce the intralaminar strength and stiffness of laminates, and even induce the delamination between layers, which results in damage to the whole bearing components. Therefore, the application of laminates in the main bearing structure is seriously restricted. Many researchers have conducted research on FRPs damage, which is called "structural health monitoring and control". Even the sensor and FRPs are integrated to monitor the damage in real time. Some structure designers allow crack propagation in laminates, but an obvious structure failure is not

**email: 15850571132@163.com*

allowed during the specified service life [4]. Hence, the crack propagation behavior of FRPs laminates is important to the damage tolerance design. Additionally, the application scope of FRPs in engineering is gradually expanding, and some special FRPs are being designed and used. In civil defense security and military engineering, the fireproof materials have attracted much attention. For instance, the mechanical behaviors of FRPs containing flame retardant need to be studied.

Rabbi et al. [5] modified the matrix by carbon nanotubes and short cut carbon fibers to prepare conductive glass fiber reinforced epoxy resin laminates (GFRP), and dynamic crack propagation experiments were performed to obtain the initial damage force and propagation states of GFRP. Zhang et al. [6] studied numerically the crack propagation of the fiber reinforced cementitious composite under tensile load by using fracture mechanics criteria, which belongs to mode I (opening type) crack. Zheng and Shen [7] established the free-volume transition theory for the deformation and fracture, and the shear banding or crack propagation in fiber-reinforced bulk metallic glasses was obtained. Tanaka et al. [8] evaluated the fatigue crack propagation in short-carbon-fiber reinforced plastics based on anisotropic fracture mechanics, the energy release rate and the stress intensity factor were derived, and the radius of crack tip region was predicted. Abd-Elhady et al. [9] investigated the fatigue crack propagation in steel pipeline repaired by glass fiber reinforced polymer. Further, the crack paths with different fiber direction were simulated by Abaqus software, and the change of stress intensity factors and J-integral ranges were obtained. Wang et al. [10] improved the stability of crack growth by coating polydopamine and graphene oxide on the surface of carbon fabric, the delamination and crack behavior were observed by double cantilever beam (DCB) and end-notched flexure (ENF) methods, and the critical strain energy release rate was drawn. Avanzini et al. [11] researched the fatigue strength and crack propagation of short carbon fiber reinforced polyetheretherketone and neat matrix with a small blind hole, which indicates that a lower fiber content and inclusion of additive particles will lower the fatigue strength and resistance to crack propagation. Jiří Vala and Vladislav Kozák [12] conducted a computational analysis of crack formation and propagation in quasi-brittle fiber reinforced composites, and a model based on the properties of fiber cementitious composites was presented. Toshiki Watanabe et al. [13] achieved the observation of crack initiation and propagation in carbon fiber reinforced epoxy resin laminates (CFRPs) by used nanoscopic SR X-CT. Their results show that the crack initiation and propagation mainly depend on the crack location and the resin thickness between fibers. And the mechanism of crack propagation can be divided into carbon fiber/resin debonding and plastic resin deformation. Hassan Ziari et al. [14] explored the crack resistance of hot mix asphalt containing different percentages of reclaimed asphalt sidewalk and glass fiber. And the fracture energy and critical J-integral in terms of temperature were developed by multiple regression model. Hyung Doh Roh et al. [15] analyzed the properties of the three-point bending and inter-laminar crack propagation of carbon fiber-reinforced plastics by electrical resistance measurement, and the FEA was conducted to verify the experiments. Dalli et al. [16] got the mode I intralaminar fracture toughness of 2D woven carbon fiber reinforced composites, the stable and unstable crack propagation were discussed by theory and simulation and experiment.

Most of the above studies have explored how to improve the interlaminar characteristics, measure crack propagation and simulate crack growth. However, the related research on continuous glass fiber reinforced epoxy resin laminates (GFRP) are rare. Especially, the crack propagation research on glass fiber reinforced epoxy resin laminates containing ammonium polyphosphate (APP) flame retardant (GFRP-APP). On this basis, the end-notched GFRP-APP specimens and a fixture were designed, and crack propagation was realized by a quasi-static single-edge tensile loading (SETL) test. Simultaneously, the tensile fracture properties of epoxy resin-casting system and 90° GFRP-APP specimens were also tested. The scanning electron microscope (SEM), X-ray diffraction (XRD) and energy dispersive spectrometer (EDS) were used to characterize the morphology of fracture face and phase composition. It will illustrate the crack propagation mechanism of GFRP-APP.

2. Materials and methods

2.1. Materials and specimens: epoxy resin and GFRP-APP

The pure epoxy resin-casting system is prepared from E-51 grades, and its classical molecular structure is shown in Figure 1a. The epoxy resin and curing agent are mixed at a mass ratio of 5:1 and then poured into the mold. The tensile test specimen can be obtained after heating to 140°C for 12 h and demoulding, as shown in Figure 2a.

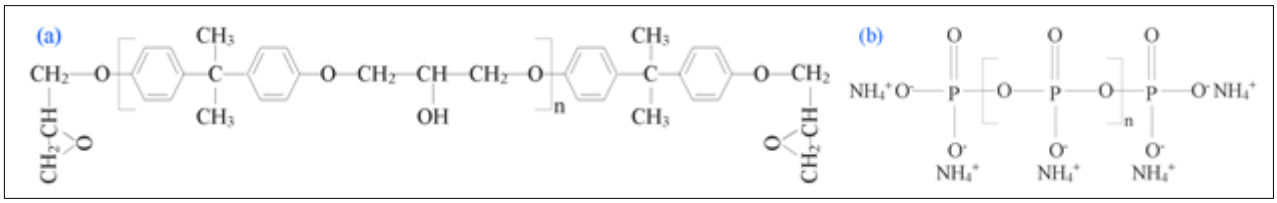

Figure 1. Molecular formula: a) epoxy resin, b) APP

GFRP-APP is prepared by flame retardant prepreg, and the high temperature hot pressing tank method is adopted. In this process, the relationship between temperature and time and pressure is shown in Figure 3. The thickness of the single layer prepreg is 0.2 mm, and the volume content of glass fiber is 34%. The flame retardant is ammonium polyphosphate, and its mass ratio is 1.49%, which molecular structure is shown in Figure 1b. The experimental specimens can be obtained by cutting the GFRP-APP laminates by water jet and drill, as shown in Figure 2 b-e. The geometry and size of the experimental specimens are shown in Figure 2. The thickness of 90° CFRP-APP tensile specimens is 2.1 mm (10 layers), and the width is 15 mm, as shown in Figure 2a. The thickness of epoxy resin tensile specimens is 4.25 mm, and the width of the standard distance section is 10.4 mm, as shown in Figure 2b. The thickness of the end-notched GFRP-APP specimens is 4.02 mm (20 layers), as shown in Figure 2c, Figure 2d and Figure 2e. Some material properties of epoxy resin and GFRP-APP are shown in Table 1 and Table 2.

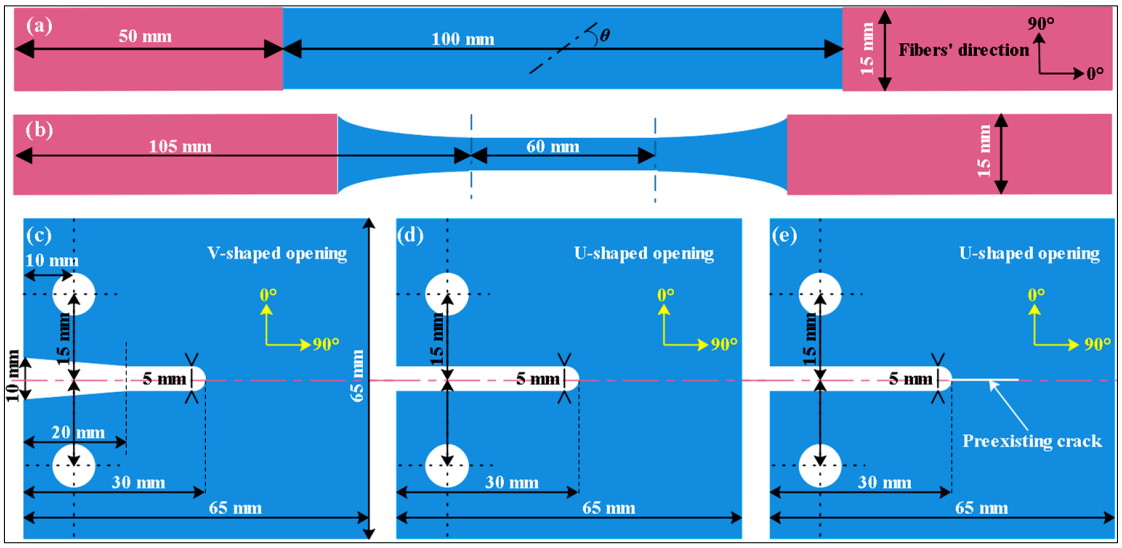

Figure 2. Type and size of specimens: a) 90° GFRP-APP, b) epoxy resin, c) V-shaped opening, d) U-shaped opening, e) U-shaped opening with preexisting crack

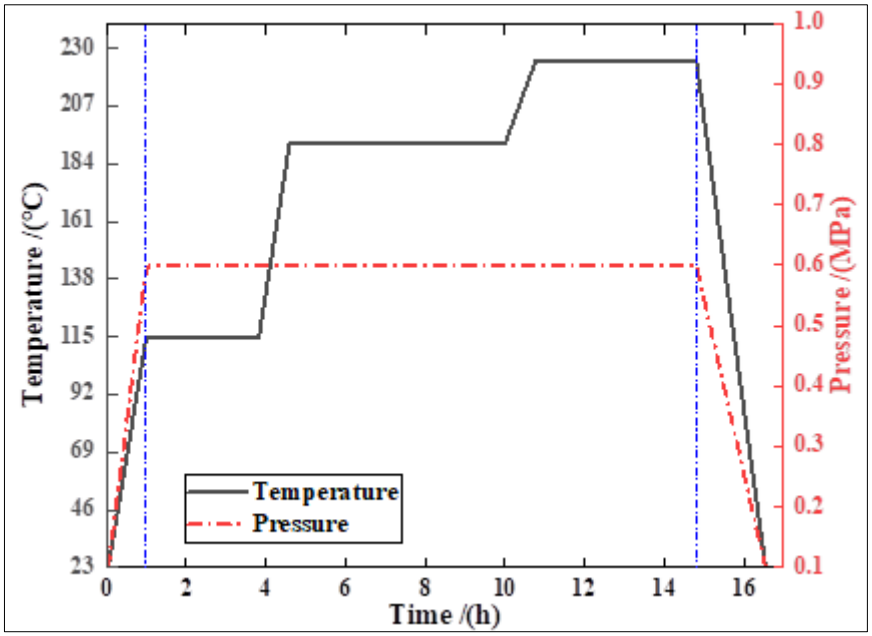

Figure 3. Temperature and pressure of the hot pressing process

Table 1. Material parameters: Epoxy resin

Sample	**Parameter**	
	Elastic modulus /*E*	Poisson's ratio /*v*
Epoxy resin	2125 MPa	0.3

Table 2. Material parameters: Single layer plate of GFRP-APP

Sample	**Parameter**		
	Elastic modulus /*E*	Shear modulus /*G*	Poisson's ratio /*v*
GFRP-APP	E_1=24.535 GPa, E_2=E_3=6.55 GPa	G_{12}=G_{23}=G_{13}=2.436 GPa	v_{12}=v_{13}=0.24, v_{23}=0.3

2.2. Experimental methods for SETL

The crack propagation of GFRP-APP laminates is mainly characterized by the intralaminar cracking and interlaminar delamination between layers. However, actually, the crack propagation are the comprehensive result of the progressive failure process of matrix, the interface debonding of fiber and matrix, and the fracture of fiber. On this basis, it is necessary to understand the mechanical characteristics of the tensile failure on matrix. The tensile experiments of 90° CFRP-APP specimens will show the mechanical behaviour of interface debonding and matrix fracture. The tensile experiments of pure epoxy resin specimens will illustrate the failure mode of matrix.

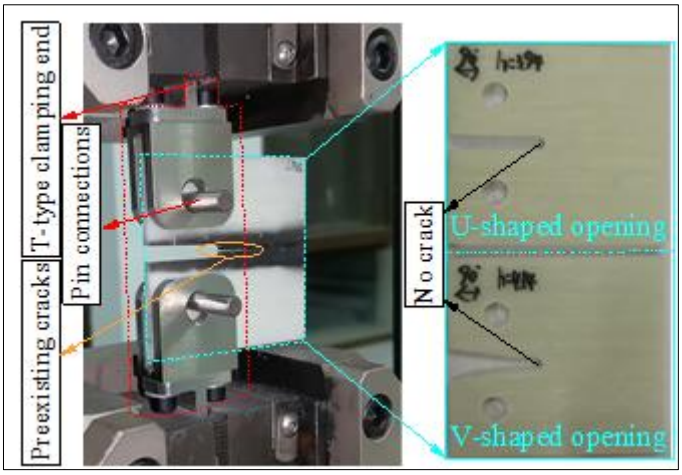

Figure 4. Fixture for opening specimen and crack propagation

In this paper, crack propagation was studied by the quasi-static SETL experiments of 90° GFRP-APP standard tensile specimens and end-notched GFRP-APP specimens. The experimental specimen types are shown in Table 3. Epoxy resin specimens are stretched at a strain rate of 0.001 s^{-1}. The 90° GFRP-APP specimens are also stretched at a strain rate of 0.001 s^{-1}. To verify the consistency of the initial force on GFRP-APP crack propagation, two kinds of specimens with U-shaped and V-shaped opening are designed, as shown in Figure 2c and Figure 2d. To obtain the progressive crack propagation, specimens with preexisting crack are prepared, such as Figure 2e. By designing the fixture (Figure 4), the SETL of end-notched specimens are realized, and the intralaminar crack propagation characteristics of unidirectional GFRP-APP can be obtained.

Table 2. Types of experiments

Samples	Types	Replicates	Loading rate	Name
Epoxy resin	Pure costing system	3	3.6 mm/min	EP
GFRP-APP	90°	3	6 mm/min	GP90
GFRP-APP	0° U-shaped preexisting crack	1	5 mm/min	GP0-U-C
GFRP-APP	0° V-shaped preexisting crack	2	5 mm/min	GP0-V-C
GFRP-APP	90° U-shaped preexisting crack	2	5 mm/min	GP90-U-C
GFRP-APP	90° U-shaped	4	5 mm/min	GP90-U
GFRP-APP	90° V-shaped	5	5 mm/min	GP90-V

3. Results and discussions

3.1. Fracture characteristics of epoxy resin and 90° GFRP-APP

The calculation method of engineering stress and strain is shown in Equation (1). The stress-strain curves and tensile fracture specimens of epoxy resin are shown in Figure 5a, and the stress-strain curves and tensile fracture specimens of 90° GFRP-APP are shown in Figure 5b. For the tensile experiments of epoxy resin, the fracture position of the first repeated experiment is the same as that of the third repeated experiment, and their fracture strength are basically the same. However, the fracture position of the second repeated experiment was different, i.e., the clamping end and middle part. It will cause the experimental error, therefore we do not consider it.

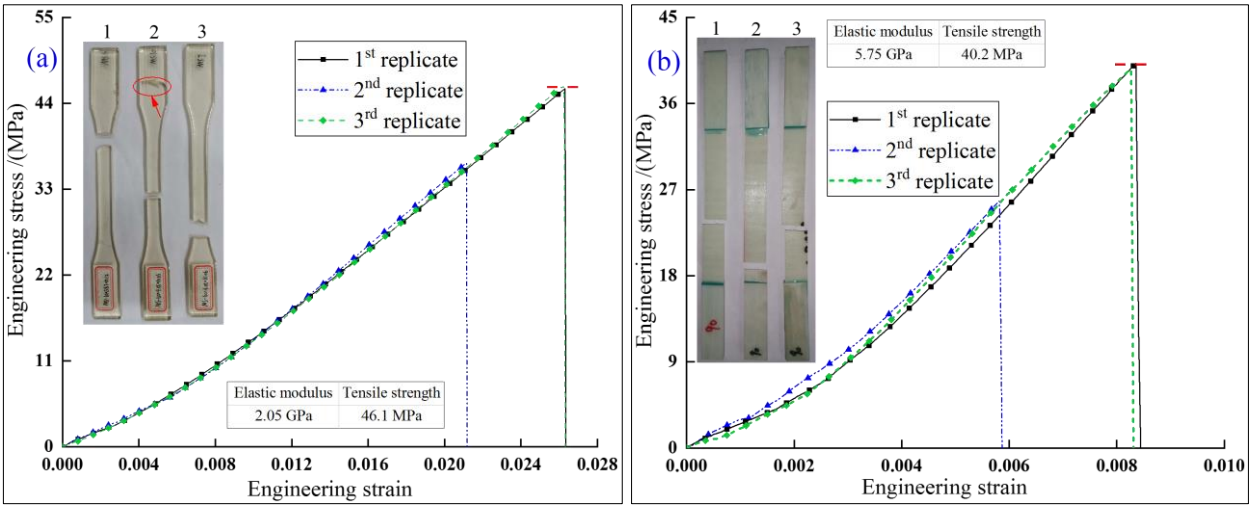

Figure 5. Experimental results of tensile fracture: a) epoxy resin, b) 90° GFRP-APP

For 90° GFRP-APP, the fracture position of the first repeated is basically the same as that of the third repeated experiment, and the fracture position of the second repeated experiment is close to the clamping end. The elastic modulus of the stress-strain curve is basically the same, but the strength limit is different. The strength limit of the second repeated experiment is much reduced, which may be caused by the initial crack in the preparation of the specimen. We always select the experimental data with a good repeatability as the research object. For epoxy resin, the elastic modulus and strength limit are 2.05 GPa and 46.1 MPa, respectively. The elastic modulus and strength limit of 90° GFRP-APP are 5.75 GPa and 40.2 MPa, respectively. Due to defects caused by machining, the experimental results are slightly lower than the factory value in Table 1 and Table 2. From the trend of their curves, the fracture characteristics of the two tensile experiments have a great similarity, both of which belong to brittle fracture.

$$\left.\begin{aligned}\sigma &= \frac{F}{A_0}\\ \varepsilon &= \frac{\Delta l}{l_0}\end{aligned}\right\} \qquad (1)$$

where F is the tensile force, and A_0 is the effective cross-section area of the specimen. l_0 is the effective length of the specimen, and Δl is the tensile distance.

3.2. Crack propagation analysis

The intralaminar crack propagation of FRPs can be divided into three forms, opening type (mode I), slip type (mode II) and tear type (mode III) [4]. During the intralaminar crack propagation process of FRPs, the special phenomenon of fiber bridge will occur after the crack tip [17-18]. The bridge region will enhance fracture toughness until it reaches to a stable value, whose phenomenon is known as the R curve [19-20]. For the end-notched 0° GFRP-APP specimens, the crack does not achieve ideal transverse propagation regardless of the opening shape. When there is no preexisting crack, it cracks directly near the U-shaped opening along 0° direction (fiber direction). When there is a preexisting crack, it cracks at the tip of preexisting crack along 0° direction (fiber direction), as shown in Figure 6a. Figure 6b showed that the end-notched 90° GFRP-APP U-shaped opening specimens without preexisting crack, and the experimental results showed the phenomenon of multi-cracks propagation. Nevertheless, in terms of 90° GFRP-APP U-shaped opening specimens with preexisting cracks, as shown in Figure 6c, it showed a fiber bridge when crack propagation. Therefore, studying the end-notched 0° specimens is inappropriate here, and the following will focus on the crack propagation of the end-notched 90° GFRP-APP specimens. According to the experimental results, the crack propagation of the end-notched 90° GFRP-APP specimens can be divided into two types. One is mode I multi-cracks propagation without preexisting crack, the other is mode I fiber bridge propagation with preexisting crack. During these pro-

pagation process, multi-cracks propagation and fiber bridge will consume more energy, which is a practical problem to be paid attention to.

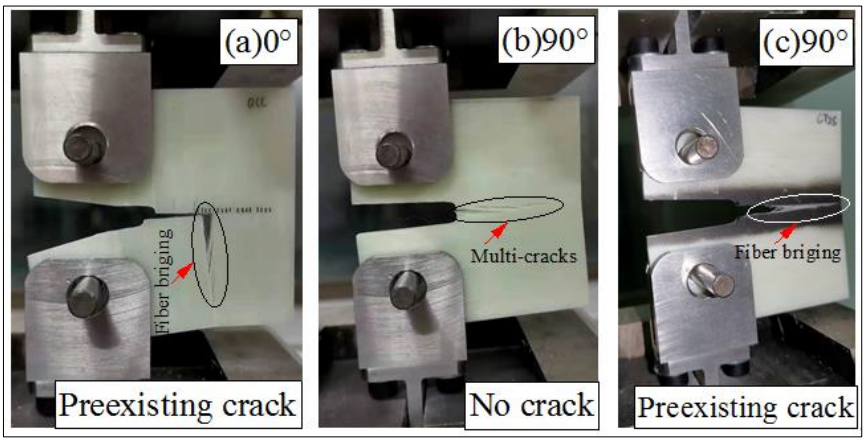

Figure 6. Experiments of crack propagation

The tensile force-opening displacement curves of crack propagation experiment are shown in Figure 7. Figure 7a showed that the crack propagation of the end-notched 0° GFRP-APP specimen is independent of opening types. The force-opening displacement curves are the same for both U-shaped and V-shaped opening, and the location of crack is along fiber direction (90°). For the end-notched 90° GFRP-APP specimens with a preexisting cracks, Figure 7b showed that the maximum force of crack birth is less than that of specimens without preexisting cracks, i.e., Figure 7c and Figure 7d. Namely, the preexisting crack effectively reduces the resistance to crack birth. The force-opening displacement curves of the preexisting crack specimens decrease exponentially slowly after crossing the peak value, which can be viewed as a progressive failure process. However, the force-opening displacement curves of the specimens without preexisting cracks decrease sharply after crossing the peak value, and then get into the progressive failure process. Here, for the specimens without preexisting crack, the failure process of crack propagation was divided into three stages, i.e., crack gestation, crack birth and crack propagation. And the specimens with preexisting crack were divided into two stages, i.e., crack gestation and crack propagation. The crack gestation means that the tensile load increases gradually until reaching the crack birth load level. When specimens have no preexisting crack, it needs to create a crack to complete the next crack propagation, and this stage was named as crack birth. In this stage, the load reduces from the crack birth load level (maximum tensile force) to a low load level. The progressive process starts here. Due to the fiber bridge effect, the tensile load of crack propagation will drop to a lower load level, and then crack propagation continues, which leads to the fracture toughness-crack length curve changes into the R curve. For fiber-polymer composites, the process of crack propagation belongs to the progressive damage behavior. The comparison of Figure 7c and Figure 7d also shows that the opening type has a great influence on the peak load, and the peak load of U-shaped opening is less than that of V-shaped opening. Perhaps this condition is related to stress concentration or machining error, etc., and we think they are all effective.

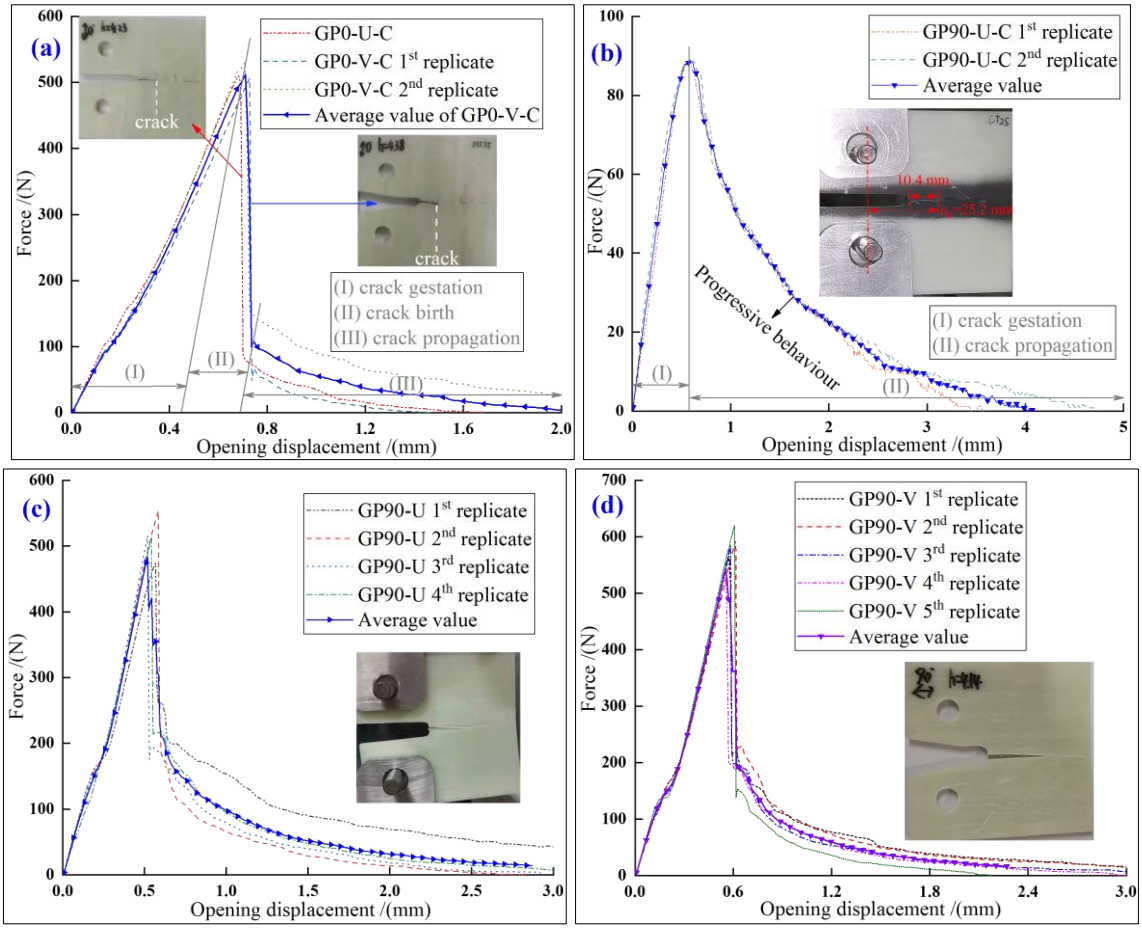

Figure 7. Experimental curves of tensile force-opening displacement

For opening specimen designed in this paper, the fracture toughness can be obtained from area method [16], which is as follows.

$$G_{IC} = \frac{1}{2t\Delta a}(P_1u_2 - P_2u_1) \tag{2}$$

where G_{IC} is the mode I fracture toughness, and it also known as mode I strain energy release rate. t is the thickness of specimen, i.e., 4.15 mm. (P_1, u_1) and (P_2, u_2) are the two peak coordinates on the force-opening displacement curve, respectively. Δa is the length of the crack propagation between two peak coordinates. Hence, the calculated mode I fracture toughness and crack birth force are shown in Table 4.

Table 4. Fracture toughness

Types of specimen	GP90-U-C	GP90-U	GP90-V
G_{IC} (N/mm)	3.059	4.211	4.184
F_{birth} (N)	89.11	483.53	544.11

Due to the crack propagation is not satisfied with the above calculation method, the fracture toughness of 0° specimens are not calculated here. The reason of low fracture toughness to preexisting crack specimens is the lack of fiber bridge, which can be used as the initial fracture toughness. The fracture toughness without preexisting crack is a stable value under fiber bridge or multi-cracks propagation. Thus, the crack birth and propagation mechanism of GFRP-APP can be roughly revealed based on the fracture energy theorem. If the crack propagation displacement is taken as the transverse coordinate, the R curve will be drawn according to the calculated fracture toughness.

3.3. Analysis of failure morphology and element phase

From the tensile experimental results Figure 5a, the pure epoxy resin belongs to brittle material and has no obvious plastic characteristics, whose failure morphology of fracture face is shown in Figure 8a. Before fracture, the crack produces from some defects (i.e., weak link), and the crack continues to propagate with the increasing of load. Many cracks and spalling gaps are formed during fracture.

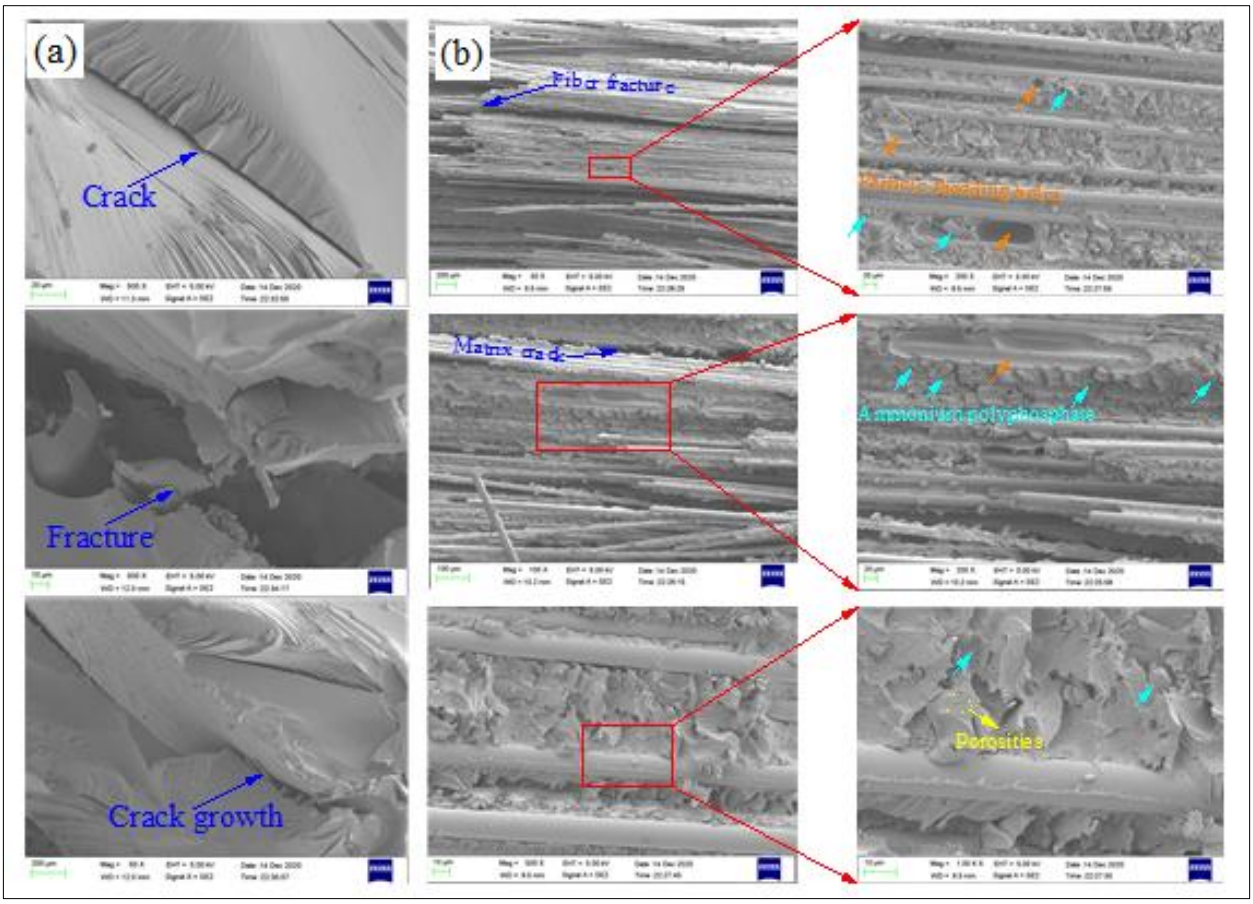

Figure 8. SEM morphology of fracture face, a) epoxy resin, b) GFRP-APP

The micro-morphology of the crack propagation fracture face of the end-notched 90° GFRP-APP is shown in Figure 8b. The failure form of crack propagation is that the matrix between fibers to be stretched and then the fiber bridge to be broken. Therefore, there will be fiber debonding, fiber pull-out and fiber fracture. Additionally, due to the addition of APP flame retardant in the matrix, the particles of APP will fall off and form some holes. Porous on the matrix can also be seen in the high power lens' SEM diagram. The porosity, fiber interface and particle interface are the inducing factors of crack propagation, and may be the factor to cause multi-cracks. Micro-cracks may propagate along the interface between the fiber and matrix, along the interface between the flame retardant and matrix, or on the matrix. Generally, the separation force of interface is less than dilaceration force of material. Therefore, it can be conjectured that the interface between the flame retardant and matrix accelerates the crack propagation speed and reduces the crack propagation resistance. The crack propagates along the interface, thus it moves around the flame retardant.

The XRD analysis and EDS analysis were performed here. By XRD analysis, the flame retardant was identified as ammonium polyphosphate. In Figure 9, the matching degree of XRD test data with the curves of known chemicals is consistent well. Glass fiber belongs to a mixture, in addition to containing silica, there are some metal oxides. According to the EDS analysis of Figure 10, a small amount of phosphorus does exist, which further determines that the flame retardant is ammonium polyphosphate. The amount of carbon element is most, combining Figure 1a, which can be determined that the carbon

element corresponding to the substance of epoxy resin. Glass fiber mainly includes silica, calcium oxide, alumina, but also contains a small amount of iron oxide and potassium oxide.

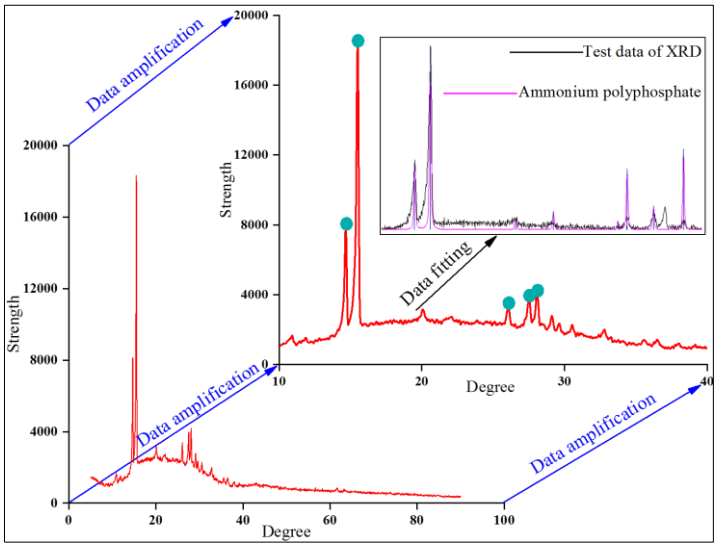

Figure 9. XRD analysis of GFRP-APP

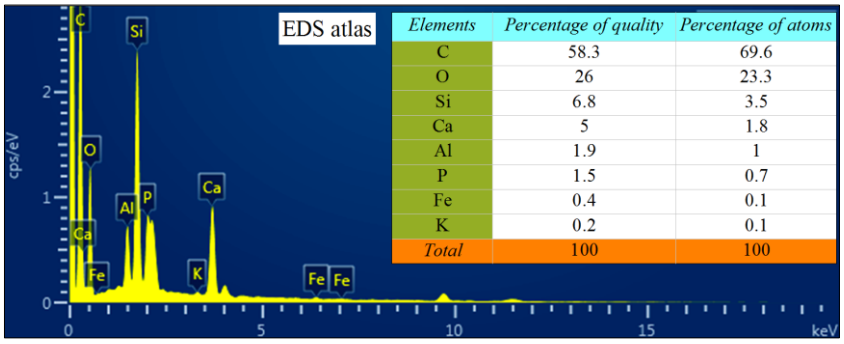

Elements	*Percentage of quality*	*Percentage of atoms*
C	58.3	69.6
O	26	23.3
Si	6.8	3.5
Ca	5	1.8
Al	1.9	1
P	1.5	0.7
Fe	0.4	0.1
K	0.2	0.1
Total	100	100

Figure 10. EDS analysis of GFRP-APP

4. Conclusions

The continuous glass fiber reinforced epoxy resin laminate containing ammonium polyphosphate flame retardant (GFRP-APP) is a kind of engineering material which is often sued in high temperature-resistant environments. Structural health analysis and damage tolerance analysis need to be obtained through numerous of experiments. Based on the single-edge tensile loading (SETL) experiments, the crack propagation behavior for end-notched GFRP-APP specimens has been studied. For the U-shaped and V-shaped opening SETL specimens, the crack propagation of the end-notched GFRP-APP belongs to mode I propagation, and includes the types of fiber bridge and multi-cracks. The crack mainly propagates along the fiber direction. In the absence of preexisting cracks, due to the lack of propagation guidance, the multi-cracks propagate simultaneously and the cross-link each other phenomenon will occur. The crack propagation of the end-notched 0° specimen is independent of opening types. The preexisting crack effectively reduce the maximum force of crack birth, and crack propagation belongs to progressive behavior. The intralaminar fracture toughness for 90° specimens of U-shaped and V-shaped opening without preexisting crack are basically the same, approximately 4.2 N/mm. The crack propagation mechanism of GFRP-APP is that the matrix between the fibers cracks under the tensile load, and then appears the fiber debonding to occur the fiber bridge phenomenon, and the fiber will be pulled out and fracture with the increasing of load. The failure forms include fracture of bridge fiber, the pull-out of fiber, and the crack of matrix. The matrix pores and interfaces are the guiding factors of crack growth. SEM analysis shows that the tensile failure of epoxy resin and 90° GFRP-APP belongs to brittle

fracture. Many pores and APP are found in the failure face. XRD analysis verifies that the flame retardant is ammonium polyphosphate. EDS analysis points out that the glass fiber composite is a kind of multi-element composite. In addition to silica, it also includes oxide impurities such as alumina, calcium oxide, iron oxide and potassium oxide.

Acknowledgements. The authors gratefully acknowledged the financial supports from the National Natural Science Foundation of China (Grant number: 12002169), the China Scholarship Council (Grant number: 202106840033), the Postgraduate Research & Practice Innovation Program of Jiangsu Province of China (Grant number: KYCX21_0342), and the 2022 Excellent Doctor Training Fund of Nanjing University of Science and Technology.

References

1.ZHAO C F, ZHOU Z T, ZHAO C X, et al. Research on Compression Properties of Unidirectional Carbon Fiber Reinforced Epoxy Resin Composite (UCFREP) [J]. *Journal of Composite Materials*, 2020. https://doi.org/10.1177/0021998320972176.

2.ZHAO C. F., LEE, H.P., GOH, K.L., et al., Preparation Process and Compression Mechanics of Carbon Fiber Reinforced Plastics Negative Poisson's Ratio Structure (CFRP+NPRS) [J]. Composite Structures, 2022, 115667. https://doi.org/10.1016/j.compstruct.2022.115667

3.ZHAO C F, ZHOU Z T, REN J, et al. Investigation of Compression Mechanics of Strain rate-dependent: Forged/Laminated Carbon Fiber-Epoxy Resin Composites [J]. *Composites: Mechanics, Computations, Applications*, 2020, 11(4): 341-367.
DOI: 10.1615/CompMechComputApplIntJ.2020033979

4.ZHAO L B, GONG Y, ZHANG J Y. A survey on delamination growth behavior in fiber reinforced composite laminates [J]. *Acta Aeronauticaet Astronautica Sinica*, 2019, 40(1): 522509-522509.
http://hkxb.buaa.edu.cn/CN/10.7527/S1000-6893.2018.22509

5.RABBI M F, MENINNO C M, CHALIVENDRA V. Damage monitoring of conductive glass fiber/epoxy laminated composites under dynamic mixed-mode fracture loading [J]. *Materials Letters*, 2020, 283. DOI: 10.1016/j.matlet.2020.128766

6.ZHANG J, LEUNG C K Y, YUAN G. Simulation of crack propagation of fiber reinforced cementitious composite under direct tension [J]. *Engineering Fracture Mechanics*, 2011.
DOI: 10.1016/j.engfracmech.2011.06.003

7.ZHENG G P, SHEN Y. Simulation of crack propagation in fiber-reinforced bulk metallic glasses [J]. *International Journal of Solids and Structures*, 2010, 47(2): 320-329.
DOI: 10.1016/j.ijsolstr.2009.10.003

8TANAKA K, OHARADA K, YAMADA D, et al. Fatigue crack propagation in short-carbon-fiber reinforced plastics evaluated based on anisotropic fracture mechanics [J]. *International Journal of Fatigue*, 2016, 92(pt.2): 415-425. DOI: 10.1016/j.ijfatigue.2016.01.015

9.ABD-ELHADY A A, ALARIFI I M, MALIK R A, et al. Investigation of fatigue crack propagation in steel pipeline repaired by glass fiber reinforced polymer [J]. *Composite Structures*, 2020, 242.
DOI: 10.1016/j.compstruct.2020.112189

10. WANG P, YANG J, LIU W, et al. Tunable crack propagation behavior in carbon fiber reinforced plastic laminates with polydopamine and graphene oxide treated fibers [J]. *Materials & Design*, 2017, 113(Jan.): 68-75. DOI: 10.1016/j.matdes.2016.10.013

11.AVANZINI A, PETROGALLI C, BATTINI D, et al. Influence of micro-notches on the fatigue strength and crack propagation of unfilled and short carbon fiber reinforced PEEK [J]. *Materials & Design*, 2017, 139(Feb.): 447-456. DOI: 10.1016/j.matdes.2017.11.039

12.JIÍ VALA, VLADISLAV KOZÁK. Computational analysis of crack formation and propagation in quasi-brittle fibre reinforced composites [J]. *Procedia Structural Integrity*, 2019, 23: 328-333.
DOI: 10.1016/j.prostr.2020.01.108

13.WATANABE, TAKEICHI Y, NIWA Y, et al. Nanoscale in situ observations of crack initiation and propagation in carbon fiber/epoxy composites using synchrotron radiation X-ray computed tomography [J]. *Composites Science and Technology*, 2020, 197: 108244.
DOI: 10.1016/j.compscitech.2020.108244
14.HASSAN ZIARI, ALIHA M R M, ALI MONIRI, et al. Crack resistance of hot mix asphalt containing different percentages of reclaimed asphalt pavement and glass fiber [J]. *Construction and Building Materials*, 230. DOI: 10.1016/j.conbuildmat.2019.117015
15.HYUNG D R, SOO-YOUNG L, EONYEON J, et al. Deformation and interlaminar crack propagation sensing in carbon fiber composites using electrical resistance measurement [J]. *Composite Structures*, 2019, 216: 142-150. https://doi.org/10.1016/j.compstruct.2019.02.100
16. DALLI D, CATALANOTTI G, VARANDAS L F, et al. Mode I intralaminar fracture toughness of 2D woven carbon fibre reinforced composites: A comparison of stable and unstable crack propagation techniques [J]. *Engineering Fracture Mechanics*, 2019. DOI:10.1016/j.engfracmech.2019.04.003
17.OZDIL F, CARLSSON L A. Beam analysis of angle-ply laminate DCB specimens[J]. *Composites Science & Technology*, 1999, 59(2): 305-315. DOI: 10.1016/S0266-3538(98)00069-4
18.IVENS J, ALBERTSEN H, WEVERS M, et al. Interlaminar fracture toughness of CFRP influenced by fibre surface treatment: Part 2. Modelling of the interface effect[J]. *Composites Science & Technology*, 1995, 54(2): 147-159. DOI: 10.1016/0266-3538(95)00049-6
19.PEREIRA A B, MORAIS A. Mode I interlaminar fracture of carbon/epoxy multidirectional laminates[J]. *Composites Science & Technology*, 2004, 64(13-14): 2261-2270.
DOI: 10.1016/j.compscitech.2004.03.001
20.DE MORAIS A B, DE MOURA M F, MARQUES A T, et al. Mode-I interlaminar fracture of carbon/epoxy cross-ply composites[J]. *Composites Science & Technology*, 2002, 62(5): 679-686.
https://doi.org/10.1016/S0266-3538(01)00223-8

Manuscript received: 22.12.2021